



# Control of fouling in a spirally-ribbed water chilled tube with electronic anti-fouling technology

Young I. Cho\*, Rong Liu

*Department of Mechanical Engineering and Mechanics, Drexel University, Philadelphia, PA 19104, USA*

Received 19 October 1998; received in revised form 10 December 1998

## Abstract

The objective of the present study was to investigate the feasibility of using electronic anti-fouling (EAF) technology to control precipitation fouling in a spirally-ribbed tube commonly used in chillers. Fouling experiments were conducted with two new tubes: one with an EAF treatment and the other without it. Brush punching of a fouled tube with an enhanced spin-grit brush cleaned almost all of the scale above the fins for the case with the EAF treatment, thus recovering 90% of the initial overall heat transfer coefficient values. However, for the case without the EAF treatment, the spin-grit brush punching was not effective in removing scale. The present experiment indicated that the EAF technology could be used to control precipitation fouling in a spirally-ribbed tube. © 1999 Elsevier Science Ltd. All rights reserved.

## 1. Introduction

When hard water is heated (or cooled) in heat transfer equipment, scaling occurs. When scale deposits on a heat exchanger surface, it is traditionally called 'fouling'. The type of scale differs from industry to industry, depending on the mineral content of the available water. One of the most common forms of scale is calcium carbonate,  $\text{CaCO}_3$  [1], which is the subject of the present study.

Once scale builds up on a heat transfer surface, at least two problems associated with scale occurs. The first problem is the degradation in the performance of the heat transfer equipment. Due to the small thermal conductivity of scale, a thin coating of scale on the heat transfer surface will greatly reduce the overall

heat transfer performance. The second less critical problem is that a small change in tube diameter substantially decreases the flow rate or increases the pressure drop across the heat transfer equipment.

Various scale-inhibiting chemicals such as dispersing or chelating agents are used to prevent scale [2]. Ion exchange and reverse osmosis are also used to reduce water hardness, alkalinity, and silica level [2]. However, these methods are expensive at the industrial level, requiring heavy maintenance for proper operation. Once fouling occurs in a heat exchanger, scale is removed by using acid chemicals, which shorten the life of heat exchanger tubes, necessitating premature replacement. When acid cleaning is not desirable, metal or nylon brushing, hydro-blasting, or sand blasting is used, operations which incur downtime and repair costs.

The present study deals with fouling problems in a spirally-ribbed tube commonly used in chillers by the air-conditioning industry. When heat transfer enhancement techniques such as spirally-ribbed tubes are used,

\* Corresponding author. Tel.: +1-215-895-2425; fax: +1-215-895-1478.

E-mail address: ycho@coe.drexel.edu (Y.I. Cho)

### Nomenclature

$A$	heat transfer surface area [ $\text{m}^2$ ] (tube OD projected area)
$\mathbf{A}$	cross-sectional area vector [ $\text{m}^2$ ]
$\mathbf{B}$	magnetic field strength vector [ $\text{N A}^{-1} \text{m}^{-1}$ ]
$d_o$	outside tube diameter [m]
$D_H$	hydraulic diameter [m]
$D_s$	inside shell diameter [m]
$\mathbf{E}$	induced electric field intensity vector [ $\text{V m}^{-1}$ ]
$Q$	heat transfer rate [W]
$R_f$	fouling resistance [ $\text{m}^2 \text{K W}^{-1}$ ], based on area of tube OD
$\mathbf{s}$	line vector along the circumferential direction [m]
$t$	time [s]
$T_{c,in}$	inlet temperature of cold water [K]
$T_{c,out}$	outlet temperature of cold water [K]
$\Delta T_{LMTD}$	log-mean-temperature-difference [K]
$U$	overall heat transfer coefficient based on outside tube diameter [ $\text{W m}^{-2} \text{K}^{-1}$ ]
$U_{clean}$	overall heat transfer coefficient at clean state [ $\text{W m}^{-2} \text{K}^{-1}$ ]

it is not clear whether the heat transfer enhancement techniques promote or reduce fouling [3]. If one considers the trapping of foulant between fins, the enhanced surface may promote the deposition rate. Furthermore, using the heat and mass transfer analogy, the mass transfer coefficient of metal ions can be greater in a ribbed tube than in a plain tube, thus also promoting the growth rate of the fouling deposit [4]. However, the enhanced surface can significantly reduce the temperature of heat transfer surface and subsequently fouling. Also, the shear stress at the enhanced surface tube can be greater than in the plain tube. Hence, the enhanced surface tube may reduce asymptotic fouling at sufficiently high fluid velocities [3,5]. In spite of the positive performance of the

enhanced surface, fouling cannot completely be prevented in a heat exchanger with enhanced surface tubes.

Hence, the real issue is whether or not any brush can indeed remove scale from an enhanced surface tube when fouling eventually occurs. If one cannot remove scale from the enhanced surface tube, the benefit of high heat transfer coefficients is short-lived.

The objective of the present study was to investigate the fouling behavior and subsequent brush cleaning performance of a spirally-ribbed tube in a laboratory condition simulating chiller operation with typical cooling tower water. It was not to compare fouling between plain and enhanced tubes. In an attempt to control precipitation fouling, an electronic anti-fouling

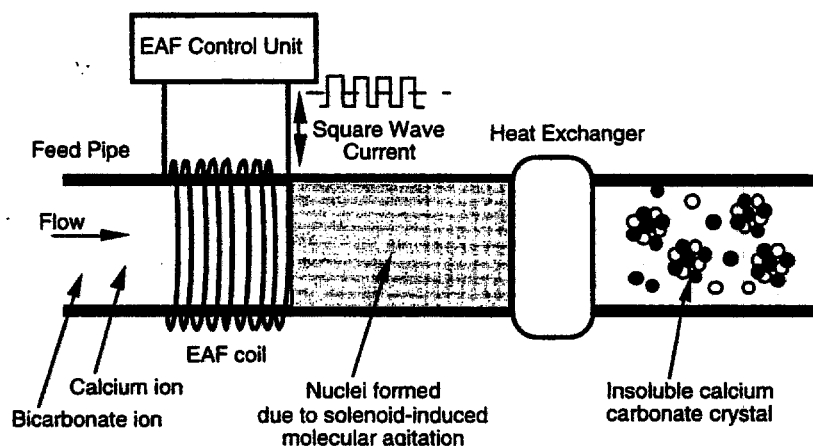


Fig. 1. Schematic diagram of the concept of electronic anti-fouling (EAF) technology. EAF control unit produces a solenoid-induced molecular agitation through Faraday's law and is installed in a feed pipe prior to heat exchanger.

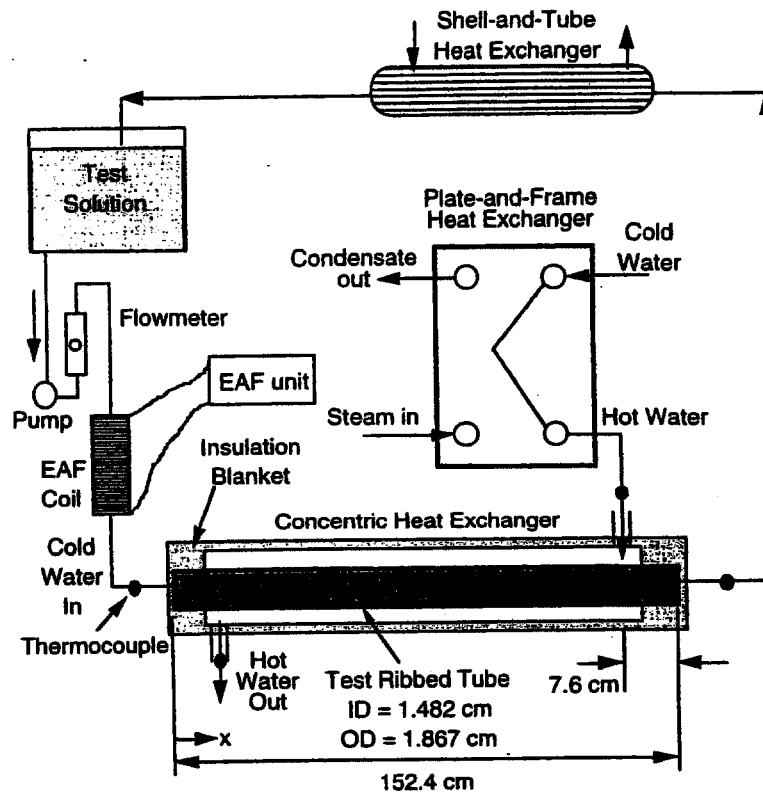


Fig. 2. Schematic diagram of recirculation-flow system with a counter-flow single-tube heat exchanger. An EAF solenoid coil is located between pump and the inlet of the main heat transfer test section.

(EAF) treatment was used. Test results will be presented for two cases: one without the EAF treatment and the other with the EAF treatment. For both cases, the fouled ribbed tube was cleaned with a new spin-grit brush, and both the  $U$  values and inside diameters were measured before and after brush punching, based on which the fouling behavior of the ribbed tubes and the benefit of using the EAF treatment were examined.

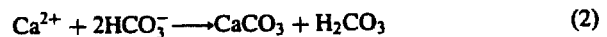
## 2. The operating principle of electronic anti-fouling technology

Fig. 1 shows a schematic diagram of the operation of an electronic anti-fouling (EAF) device. A wire is wrapped around a feed pipe to a heat exchanger, forming a solenoid. The two ends of the wire are connected to an EAF control unit. The EAF unit produces a pulsing current to create a time-varying magnetic field inside the pipe. Subsequently, the time-varying magnetic field creates an induced electric field inside the pipe, a phenomenon which can be described by Faraday's law [6]:

$$\int \mathbf{E} \cdot d\mathbf{s} = -\frac{\partial}{\partial t} \int \mathbf{B} \cdot d\mathbf{A} \quad (1)$$

In order to maximize the induction, a pulsing current having a square-wave signal is used. The current and frequency of the square-wave signal used in the present study were 0.2 A and 500 Hz, respectively. More descriptions on the use of the electronic anti-fouling technology can be found elsewhere [7-11].

The induced electric field, which oscillates with time, provides molecular agitation to charged mineral ions such that dissolved mineral ions such as calcium and bicarbonate collide and precipitate with the help of impurities in water (e.g., iron oxide particles), forming  $\text{CaCO}_3$  nuclei, see Fig. 1.



As fluid temperature increases inside a heat exchanger, the  $\text{CaCO}_3$  nuclei particles grow to large crystals, further consuming dissolved mineral ions, thus reducing both the diffusion and reaction of the ions on the heat transfer surface. Subsequently, new fouling can be mitigated or prevented. The concept of introdu-

cing fine particles to reduce fouling is not new. Troup and Richardson [12], who reviewed both chemical and physical methods of water treatment used to prevent fouling in heat exchangers, reported that fouling could be reduced by simply feeding fine  $\text{CaCO}_3$  particles or forming  $\text{Al}(\text{OH})_3$  particles in solution using aluminum electrodes across which an alternating current was passed.

### 3. Experimental method

Fig. 2 schematically shows the test facility which consists of a reservoir tank, a pump, a flow meter, an electronic anti-fouling control unit, a solenoid coil wrapped around a pipe, the main heat transfer test section, a plate-and-frame heat exchanger, and a shell-and-tube heat exchanger.

The main heat transfer test section was made of two concentric tubes, which formed a counter-flow heat exchanger. The tube was made of a spirally-ribbed tube (Wolverine Turbo CII), commonly used in a chiller by the air-conditioning industry. The shell side diameter ( $ID$ ) was 2.54 cm, whereas the ribbed tube inside and outside diameters were 1.482 and 1.867 cm, respectively. The total axial length of the tube was 1.524 m, and the actual heat transfer section inside the heat exchanger was 1.3716 m. Two reducing unions were used at both the inlet and outlet of the heat exchanger for easy connection between the heat exchanger and connecting tubes. Hard (cold) water was pumped into the tubeside, whereas hot water moved through the shellside, resulting in scale-deposits on the inside wall of the ribbed tube.

Since the hardness of tap water available in Philadelphia is approximately  $1.4 \text{ mol m}^{-3}$  as  $\text{CaCO}_3$ , it is not suitable for fouling experiments. Note,  $1 \text{ mol m}^{-3}$  is equal to  $100 \text{ mg l}^{-1}$  for  $\text{CaCO}_3$ . Therefore, artificially hardened water of  $7.5 \text{ mol m}^{-3}$  was prepared in a 200 liter tank by adding 166.5 g of calcium chloride and 252 g of sodium bicarbonate to the tank. Because of the deposition of  $\text{CaCO}_3$ , the water hardness decreased with time. After 12 h of operation, 166.5 g of calcium chloride and 252 g of sodium bicarbonate were added again.

The inlet temperature of the hard water was maintained at  $308 \pm 0.5 \text{ K}$  during the scale build-up process for the present tests. Tubeside flow rate during the scale build-up process was kept at  $11.356 \times 10^{-5} \text{ m}^3 \text{ s}^{-1}$  (i.e.,  $1.8 \text{ U.S. gal min}^{-1}$ ), which resulted in the tubeside velocity of  $0.658 \text{ m s}^{-1}$ . The corresponding Reynolds number was 9870. It is of note that the viscosity and density of the test water used in the Reynolds number calculation were evaluated at the average temperature of the water. Since the present study investigated the effect of brush punching on the



Enhanced Spin-Grit Brush

### ESGB Brushes Are for Use in Internally Enhanced Tubes

Fig. 3. Photograph of enhanced spin-grit brush (Goodway).

removal of scale, this relatively low flow velocity of  $0.658 \text{ m s}^{-1}$  was chosen to ensure scale build-up at the laboratory. Note that the minimum flow velocity for the standard chiller design in the air-conditioning industry is approximately  $1.0 \text{ m/s}$ .

Two fouling experiments were conducted following the above scale build-up process: the first one under relatively severe fouling conditions and the second under less severe fouling conditions. The temperature of the hot water entering shellside was  $338 \pm 1.0 \text{ K}$  for the first test, and  $323 \pm 1.0 \text{ K}$  for the second test, whereas shellside flow rate was kept constant at 5 GPM for the first test and 6 GPM for the second test. The hot water was continuously produced using high pressure steam provided by the Philadelphia city steam network in a plate-and-frame heat exchanger.

Thermocouples used in the present study were Omega model TMTSS-125G-6 (grounded copper-constantan T type). Calibration was carried out at 273 and 373 K, confirming the manufacturer's claim of the accuracy of  $\pm 0.1 \text{ K}$ . Flow meters were also calibrated over a range of flow rates by measuring the weight of water accumulated over time, and the calibration results were reported elsewhere [13].

After the scale was produced inside two ribbed tubes under identical conditions except that the water in one tube (#2) was treated by the EAF unit, the overall heat transfer coefficient ( $U$  value) and inside tube diameter were measured for both tubes. Scale thickness was obtained by measuring the inside tube diameter with a bore micrometer (Brown and Sharp INGAGE Internal Bore Micrometer Model 78.110602 with 6-in. extensions) at eight different axial positions over the ribs. Then, the two tubes were cleaned using a Goodway RAM-4 tube cleaner with an enhanced spin-grit brush (by Goodway ESGB-062), as shown in Fig. 3. Two punches from the inlet side and two punches from the outlet side were applied for this cleaning. After brush cleaning, both the  $U$  value and inside diameter were measured again.

The effectiveness of the EAF treatment was evaluated by comparing the changes in both the inside diameter and  $U$  value. Since the inlet temperature of the cold water influences the magnitude of the overall heat

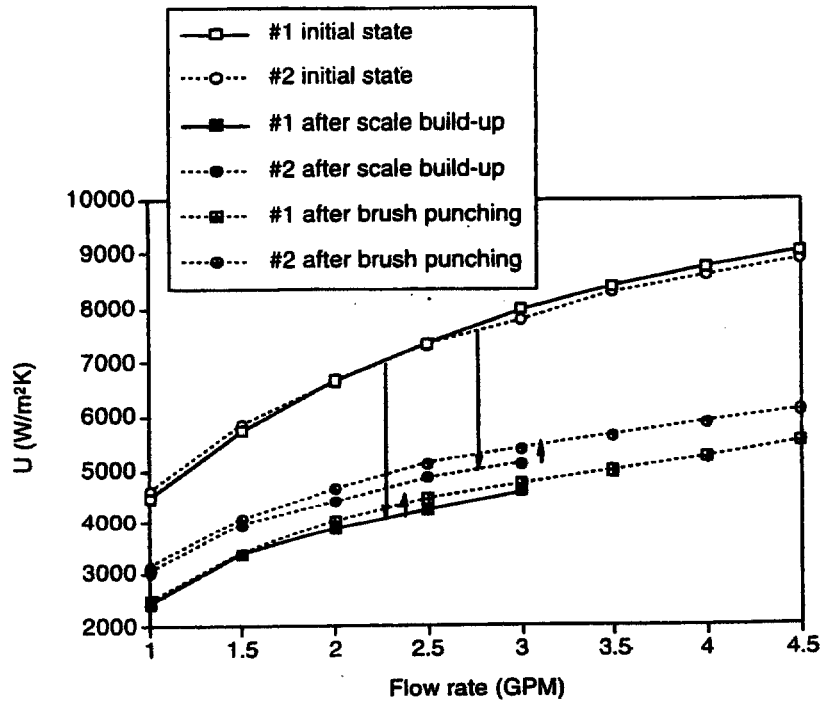


Fig. 4. Overall heat transfer rate vs flow rate after scale build-up for relatively severe fouling condition. #1 tube is for untreated case and #2 tube is EAF treated case. Note:  $1 \text{ W/m}^2 \text{ K} = 0.1762 \text{ Btu/h-ft}^2 \text{ }^\circ\text{F}$ .

transfer coefficient [14], all  $U$  value measurements were carried out with an inlet temperature of the cold tap water at  $298 \pm 0.4 \text{ K}$  in a range of flow rates of 1-4.5

GPM in the present study. The flow velocity and Reynolds number corresponding to 4.5 GPM were 1.645 m/s and 24,675, respectively.  $U$  values were cal-

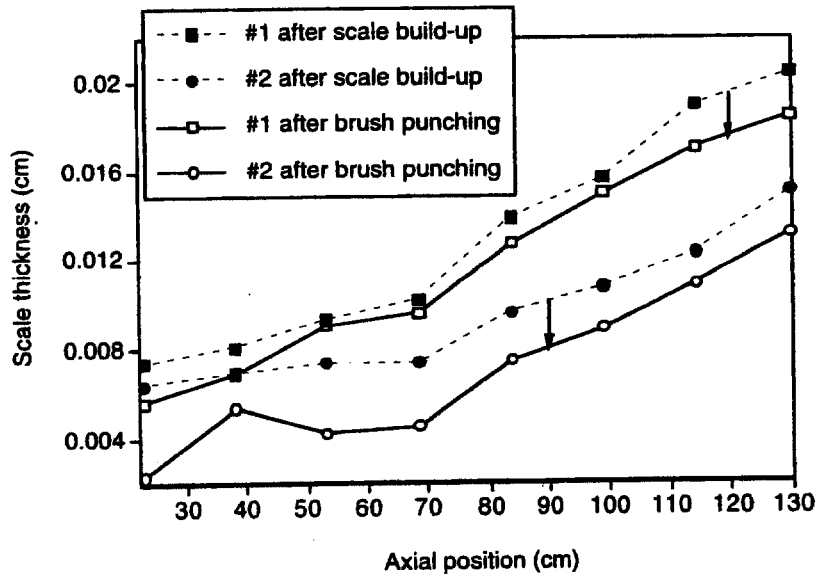


Fig. 5. Scale thickness vs axial distance after scale build-up and brush punching for relatively severe fouling condition. #1 tube is for untreated case and #2 tube is EAF treated case.

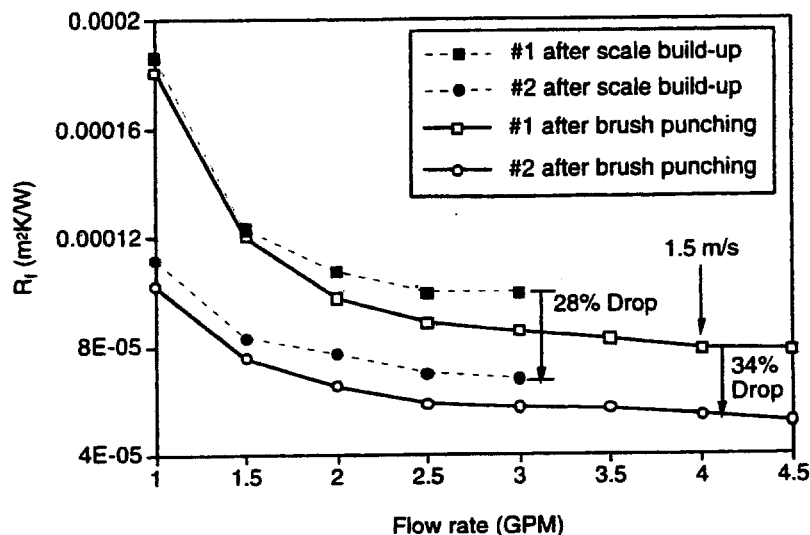


Fig. 6. Fouling resistance vs flow rate for moderate fouling condition. #1 tube is for untreated case and #2 tube is EAF treated case. Note:  $1 \text{ m}^2 \text{ K/W} = 5.68 \text{ h-ft}^2 \text{ }^\circ\text{F/Btu}$ .

culated using the log-mean-temperature-difference (LMTD) method [15]. The log-mean-temperature-difference,  $\Delta T_{\text{LMTD}}$ , was obtained from the four temperatures measured at both the inlet and outlet of cold and hot streams.

$$Q = UA\Delta T_{\text{LMTD}} = \dot{m}_c C_p (T_{c,\text{out}} - T_{c,\text{in}}) \quad (3)$$

$$U = \frac{\dot{m}_c C_p (T_{c,\text{out}} - T_{c,\text{in}})}{A\Delta T_{\text{LMTD}}} \quad (4)$$

Note that the value of the heat transfer surface area,  $A$ , was determined by normal projected area at the outside diameter of ribbed tube, which was 1.867 cm. Fouling resistance,  $R_f$ , was calculated using the usual definition [16]

$$R_f = \frac{1}{U(t)} - \frac{1}{U_{\text{clean}}} \quad (5)$$

where  $U(t)$  and  $U_{\text{clean}}$  are the overall heat transfer coefficients corresponding to fouled and initial clean states, respectively. The errors estimated from the uncertainty analysis for  $Q$ ,  $U$ ,  $R_f$  and  $A$  (heat transfer surface area) were 2.5, 2.8, 7.7 and 1.1%, respectively.

#### 4. Results and discussion

Figs. 4-6 present test results obtained from the first series of fouling experiments conducted under relatively severe fouling conditions. Fig. 4 shows  $U$  values as a function of flow rate in both the clean and fouled states for the two different tube cases: one without the

EAF treatment (designated as #1 tube), and the other with it (designated as #2 tube). In the clean state, the  $U$  values of both tubes were basically the same. After the scale build-up process, the  $U$  values were measured again over a range of flow rates of 1-3 GPM. A higher flow rate than 3 GPM was not used for fear of scale being removed, an operation which might have altered inside diameter data. The  $U$  values in the untreated tube #1 dropped by 42% from the initial  $U$  value, whereas the  $U$  value in the treated tube #2 dropped by 34%. Subsequent brush punching with a spin-grit brush increased the  $U$  values by approximately 5% for both tubes.

Fig. 5 represents scale thickness measured over the ribs as a function of axial distance for both tubes. At the beginning of each test, the inside diameter of a clean new tube was measured at eight axial locations. The average inside diameter of the clean ribbed tube was 1.482 cm. In other words, the tip of spiral fins is the reference point of scale thickness measurements. After scale was produced, the inside diameters were measured again at the eight axial locations, and the scale thickness was thus determined. Because water was heated inside the tube, the outlet temperature was higher than the inlet temperature, rendering more scale near the outlet. For example, scale thickness was 0.00737 cm near the inlet and 0.0204 cm near the exit for the untreated tube #1, whereas the corresponding scale thickness for the treated tube #2 was 0.00635 cm and 0.01352 cm, respectively, before punching. The scale thickness with the EAF treatment was approximately 33% less than without the EAF treatment near the outlet.

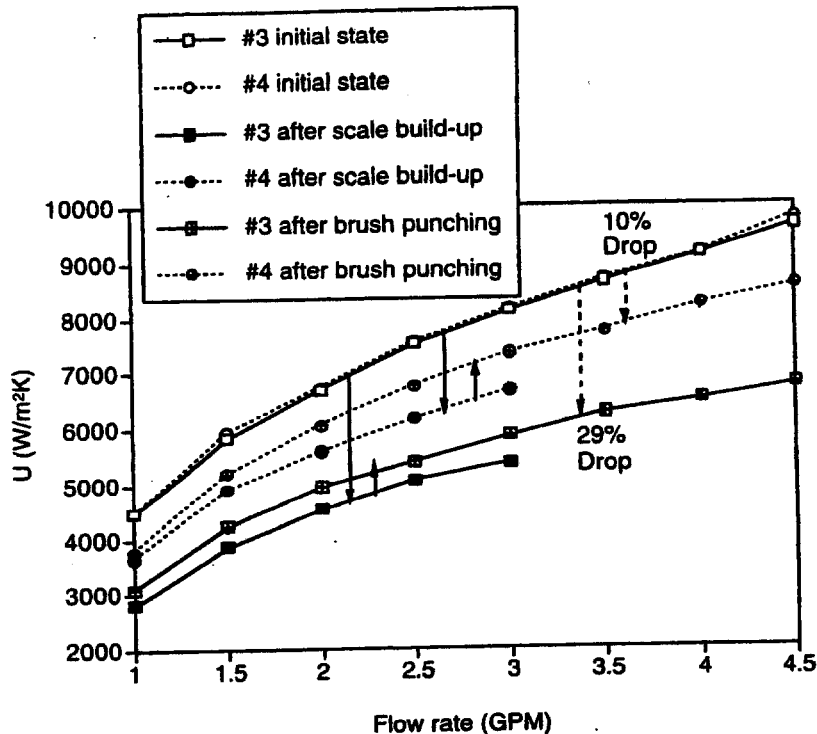


Fig. 7. Overall heat transfer rate vs flow rate after scale build-up for moderate fouling condition. #3 tube is for untreated case and #4 tube is EAF treated case. Note:  $1 \text{ W/m}^2 \text{ K} = 0.1762 \text{ Btu/h-ft}^2 \text{ }^\circ\text{F}$ .

Scale thickness results measured after brush punching show that the treated tube #2 was cleaned better with the spin-grit punching than the untreated tube #1.

Fig. 6 shows fouling resistance results of the first fouling tests for the two tubes before and after brush punching. Fig. 6 clearly depicts that the EAF treatment renders smaller fouling resistances. The fouling resistance for the treated tube #2 before punching was 28% less than the untreated tube #1. Furthermore, the fouling resistance for the treated tube #2 after punching was 34% less than the untreated tube #1.

One interesting observation in Fig. 6 is that the fouling resistance varied with flow rates when it was calculated based on the changes in  $U$  values using Eq. (5), although the amount of scale on the heat transfer surface did not change. Traditionally, the fouling resistance,  $R_f$ , is defined as

$$R_f = \frac{x}{k_f} \quad (6)$$

where  $x$  and  $k_f$  are the thickness and thermal conductivity of scale, respectively. According to Eq. (6), the fouling resistance must be constant for a given fouling condition and cannot vary with flow rates. The authors believe that the above definition of the fouling resistance, Eq. (6), should be used with care.

The results in Fig. 6 clearly depict that the fouling resistance of a heat exchanger reaches an asymptotic value at high flow velocities (i.e., greater than 1.5 m/s) so that the use of a constant fouling resistance is justified at high flow velocities. However, when the flow velocity in a heat exchanger is small (i.e., less than 1.0 m/s), the actual fouling resistance is significantly greater than the asymptotic value obtained at high velocities. In other words, the actual  $U$  value that can be obtained from the heat exchanger is much smaller than the design capacity based on the asymptotic fouling resistance.

Recently, Cho et al. [14] reported that fouling resistance is critically affected by the inlet temperature of cooling water. Even when there is no change in the actual fouling conditions inside a heat exchanger, the overall heat transfer coefficient decreases in winter, resulting in an increased fouling resistance. Typically, there is an approximately 25% increase in the fouling resistance from summer to winter in a shell-and-tube heat exchanger. When one examines the fouling resistance results without considering the seasonal effect, one may conclude erroneously that fouling actually occurs during winter and that it somehow disappears miraculously during summer, a phenomenon which has caused serious concerns among plant operating engin-

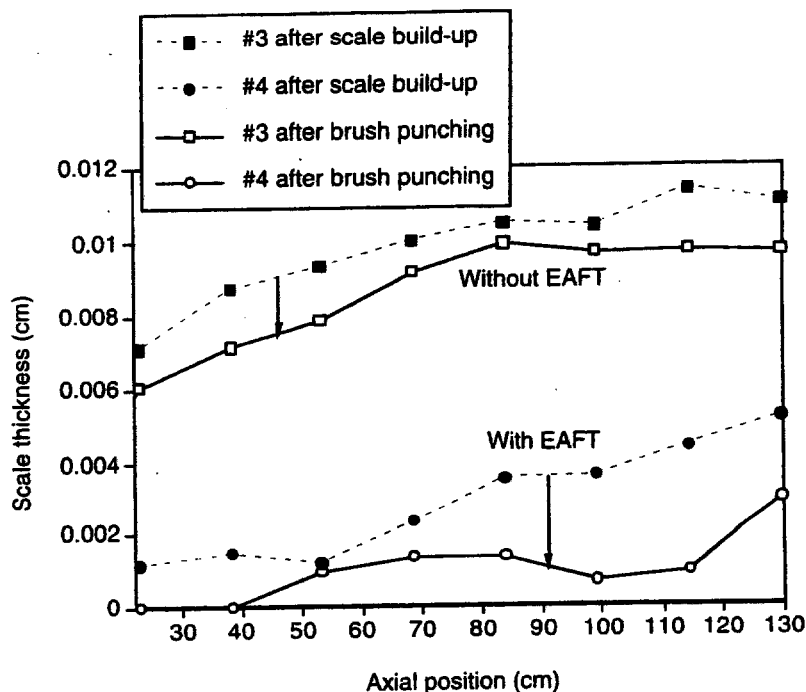


Fig. 8. Scale thickness vs axial distance after scale build-up and brush punching for moderate fouling condition. #3 tube is for untreated case and #4 tube is EAF treated case.

eers. This is another good example showing that the definition of the fouling resistance as given in Eq. (6) is insufficient and misleading.

Figs. 7-9 present test results obtained from the second series of fouling experiment which used less severe

fouling conditions than the first series of the experiment. Fig. 7 shows  $U$  values as a function of flow rate in both the clean and fouled states for the two different tube cases: one without the EAF treatment (designated as #3 tube) and the other with it (designated as #4

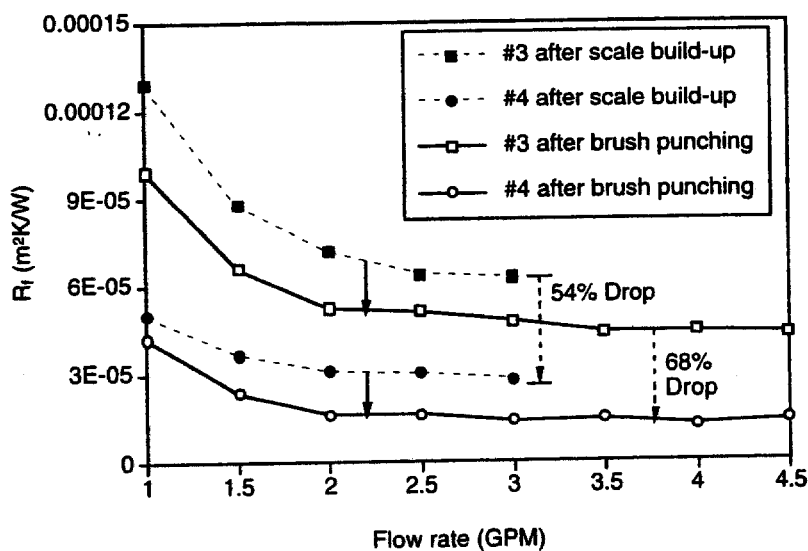


Fig. 9. Fouling resistance vs flow rate for relatively severe fouling condition. #3 tube is for untreated case and #4 tube is EAF treated case. Note:  $1 m^2 K/W = 5.68 h-ft^2 \text{ } ^\circ F/Btu$ .



tube). In the clean state, the  $U$  values of both tubes were basically the same. After the scale build-up process, the  $U$  values were measured again over a range of flow rates of 1–3 GPM. Fig. 7 shows that the  $U$  values in the untreated tube (#3) dropped to 66% of the initial  $U$  value, whereas the  $U$  value in the treated tube (#4) dropped to 82% level. Subsequent brush punching with the spin-grit brush increased the  $U$  values to 71% of the initial  $U$  value for the untreated tube (#3), whereas it restored to 90% of the initial  $U$  value for the treated tube (#4).

Fig. 8 represents scale thickness as a function of axial distance for both tubes after scale build-up and brush punching. The scale thickness after scale build-up process was 0.00711 cm near the inlet and 0.0110 cm near the exit for the untreated tube #3, whereas the corresponding scale thickness for the treated tube #4 was 0.00114 cm and 0.00521 cm, respectively. The scale thickness in the tube with the EAF treatment was approximately 53% less than without the EAF treatment near the outlet.

Scale thickness results measured after brush punching show that the scale from the treated tube (#4) was almost completely removed beyond the fins, whereas the scale from the untreated tube (#3) was hardly removed as depicted by open square symbols in Fig. 8.

Fig. 9 shows fouling resistance results for the two tubes before and after brush punching. Fig. 9 clearly depicts that the EAF treatment renders much smaller fouling resistances. The fouling resistance for the treated tube #4 before punching was  $2.76 \times 10^{-5} \text{ m}^2 \text{ K/W}$ , whereas that for the untreated tube was  $6.22 \times 10^{-5} \text{ m}^2 \text{ K/W}$ , indicating that the fouling resistance for the treated tube was 54% less than the untreated tube #4. Furthermore, the fouling resistance for the treated tube #4 after punching was 68% less than the untreated tube #4.

## 5. Conclusions

The present study was conducted in order to investigate whether or not the combined use of an electronic anti-fouling technology and brush cleaning can effectively remove scale from a spirally-ribbed tube commonly used in a chiller. When an electronic anti-fouling (EAF) treatment was applied during the normal operation of a chiller, new scale build-up was significantly less compared with the case without the EAF treatment. Subsequent brush punching with an enhanced spin-grit brush recovered 90% of the initial  $U$  value. One of the reasons why the combined use of the EAF treatment and enhanced spin-grit brush punching did not recover 100% of the initial  $U$  value was that the foulant between the fins could not totally be removed with the enhanced spin-grit brush.

However, when the EAF treatment was not used, the spin-grit punching did not effectively remove scale from the ribbed chiller tube. In other words, without EAF treatment one can make only a marginal difference in overall heat transfer coefficient due to brush cleaning and in fact never return a chiller to original performance once the  $U$  value is reduced by 30–40% due to fouling. This is not good news for those using internally enhanced tubes. Currently, fouling tests are being conducted with various brushes and techniques and the results will be reported in the future.

## Acknowledgement

The authors wish to acknowledge Mr Keith Starner at York International (York, PA) for his helpful information on ribbed water-chilled tube and his helpful comments on this paper.

## References

- [1] J.C. Cowan, D.J. Weintritt, *Water-Formed Scale Deposits*, Gulf Publishing Company, Houston, TX, 1976.
- [2] G. Tchobanoglous, F. Burton, *Wastewater Engineering, Treatment, Disposal and Reuse*, McGraw-Hill, New York, 1991.
- [3] E.F.C. Sommerscales, A.E. Bergles, Enhancement of heat transfer and fouling mitigation, in: T.F. Irvine Jr, et al. (Eds.), *Advances in Heat Transfer*, vol. 30, Academic Press, New York, 1997, pp. 197–253.
- [4] D. Hasson, H. Sherman, M. Biton, Prediction of Calcium Carbonate Scaling Rates, *Proceedings of the 6th International Symposium Fresh Water from the Sea 2* (1978) 193–199.
- [5] A.P. Watkinson, L. Louis, R. Brent, Scaling of enhanced heat exchanger tube, *The Canadian J. of Chem. Eng.* 52 (1974) 558–562.
- [6] R.A. Serway, in: *Physics for Scientists and Engineers*, 3rd ed., Saunders College Publishing, Philadelphia, PA, 1990, pp. 874–891.
- [7] Y.I. Cho, C. Fan, B.G. Choi, Theory of electronic descaling technology of control precipitation fouling in heat exchangers, *Int. Comm. Heat Mass Transfer* 24 (1997) 747–756.
- [8] Y.I. Cho, B.G. Choi, B.J. Drazner, Use of electronic descaling technology to control precipitation fouling in plate-and-frame heat exchangers, in: R.K. Shah (Ed.), *Compact Heat Exchangers for the Process Industries*, Begell House, New York, 1997, pp. 267–273.
- [9] Y.I. Cho, B.G. Choi, B.J. Drazner, Electronic anti-fouling technology to mitigate precipitation fouling in plate-and-frame heat exchangers, *Int. J. Heat Mass Transfer* 41 (1998) 2565–2571.
- [10] Y.I. Cho, B.G. Choi, Effect of fouling on temperature